AMERICAN UNIVERSITY OF BEIRUT

A NOVEL M-CYCLE EVAPORATIVE COOLING VEST FOR ENHANCED COMFORT OF ACTIVE HUMAN IN HOT ENVIRONMENT

by

RAGHEB HASSAN RAAD

A thesis

submitted in partial fulfillment of the requirements

for the degree of Master of Engineering

to the Department of Mechanical Engineering

of the Faculty of Engineering and Architecture

at the American University of Beirut

Beirut, Lebanon

September 2018

AMERICAN UNIVERSITY OF BEIRUT

A NOVEL M-CYCLE EVAPORATIVE COOLING VEST FOR ENHANCED COMFORT OF ACTIVE HUMAN IN HOT ENVIRONMENT

by
RAGHEB RAAD

Approved by:

Dr. Kamel Abou Ghali, Professor & Chair [Signature] Advisor
[ME]
(as listed in AUB Catalogue of current year)

_Dr. Nesreene Ghaddar, Professor [Signature]
[ME] Member of Committee

___Dr. Ali Tehrani, Assistant Professor [Signature]
[Chemical Engineering] Member of Committee

Date of thesis/dissertation defense: [September 14, 2018]

AMERICAN UNIVERSITY OF BEIRUT

THESIS, DISSERTATION, PROJECT RELEASE FORM

Student Name: Raad (Last) Ragheb (First) Hassan (Middle)

◉ Master's Thesis ○ Master's Project ○ Doctoral Dissertation

☐ I authorize the American University of Beirut to: (a) reproduce hard or electronic copies of my thesis, dissertation, or project; (b) include such copies in the archives and digital repositories of the University; and (c) make freely available such copies to third parties for research or educational purposes.

☑ I authorize the American University of Beirut, to: (a) reproduce hard or electronic copies of it; (b) include such copies in the archives and digital repositories of the University; and (c) make freely available such copies to third parties for research or educational purposes after :

One ---- year from the date of submission of my thesis, dissertation, or project.
Two ---- years from the date of submission of my thesis, dissertation, or project.
Three ---- years from the date of submission of my thesis, dissertation, or project.

Ragheb — September 17, 2018

Signature Date

This form is signed when submitting the thesis, dissertation, or project to the University Libraries

ACKNOWLEDGMENTS

I would like to thank my advisors, Professor Kamel Ghali and Professor Nesreene Ghaddar.

I would also like to Dr. Mariam Itani for her help in the work.

I would also like to show deep gratitude and appreciation to my family members and friends for their support throughout the past years, especially my sister Petra, my dad Hassan, and my mom Zannoubia Krayem. Nothing was possible without them.

This publication was made possible by the Collaborative Research Stimulus grant award 24477-103557 of the American University of Beirut. The findings achieved herein are solely the responsibility of the authors.

AN ABSTRACT OF THE THESIS OF

Ragheb Hassan Raad for Master of Engineering

Major: Mechanical Engineering

Title: A Novel M-Cycle Evaporative Cooling Vest for Enhanced Comfort of Active Human in Hot Environment

The long exposure of workers to hot and humid environments increases their discomfort and exposes them to excessive sweating, affecting their performance. Comfortable cooling vests are potential solutions to increase the productivity of the workers. This study suggests a vest that cools the back based on the indirect evaporative cooling technique, the Maisostsenko cycle (M-cycle), under which the air is cooled sensibly before it is evaporatively cooled. The cooling performance of the suggested vest is compared to a control vest that is based on the direct evaporative cooling technique. Computational models of the two vests are developed and verified by conducting experiments at 36 ± 0.5°C and 43 ± 2% on a heated plate, providing a constant heat flux. The simulations and the experiments showed that the M-cycle cooling technique extracts more moisture than the direct evaporative cooling one. The mathematical models of both cooling techniques were then coupled with a validated bioheat model which allowed studying the human thermal and comfort responses to the proposed designs. Ambient air conditions and the activity level served as input to the computations that will predict the back torso skin temperature and overall thermal comfort under the two vest designs. The results showed that the M-cycle vest would indeed lead to a lower back temperature by a maximum of 1.27°C, and better thermal comfort for the wearer by a maximum of 38%. This improvement in thermal comfort was more noticeable at higher ambient temperature of 45°C and lower ambient relative humidity of 18%.

CONTENTS

NOMENCLATURE

A	area (m^2)
C_p	specific heat (J/kg·K)
h_d	convective heat transfer coefficient in dry channel ($W/m^2 \cdot K$)
h_{fg}	heat of condensation (J/kg)
h_m	mass transfer coefficient ($kg/m^2 \cdot kPa \cdot s$)
h_w	convective heat transfer coefficient in wet channel ($W/m^2 \cdot K$)
$\dot{m}$	air mass flow rate (kg/s)
m_{acc}	mass of sweat accumulated per unit are of the skin (kg/m^2)
R_e	evaporative resistance of the fabric
RH	relative humidity
T	temperature (°C)
t	time (s)
V	flow velocity (m/s)
w	humidity ratio (g/kg_a)
A	area (m^2)
C_p	specific heat (J/kg·K)
h_d	convective heat transfer coefficient in dry channel ($W/m^2 \cdot K$)
h_{fg}	heat of condensation (J/kg)
h_m	mass transfer coefficient ($kg/m^2 \cdot kPa \cdot s$)
h_w	convective heat transfer coefficient in wet channel ($W/m^2 \cdot K$)

Greek Symbols

δ	thickness of the channel
ρ	density (kg/m^3)

Subscripts

a	microclimate air
d	dry channel
hf	hygroscopic fabric
p	conductive plate
sk	skin layer
w	wet channel
a	microclimate air

ILLUSTRATIONS

Figure

TABLES

Table

CHAPTER I

NOVEL M-CYCLE EVAPORATIVE COOLING VEST.

A. Introduction

When performing activities in hot environments, the human body has its own mechanisms to thermo-regulate its temperature by vasodilation and sweating. Cooling is achieved through these mechanisms to keep the core body temperature within a narrow and acceptable range to allow normal functioning of the internal organs. However, in hot environments, it is difficult for the body to maintain a stable core temperature without the aid of external cooling. In such environments, outdoor workers may be at risk of strains and heat which could lead to severe problems (Yi and Chan, 2017). The direct consequences of uncompensated heat stress include the loss of efficiency and productivity. Prolonged heat stress exposures lead to long-term effects which are noted by a progressive loss of performance capability, disorganized nervous system activity, heat illnesses and heat injuries (Miller and Bates, 2007). Some of the illnesses caused by heat stress include heat cramps, heat exhaustion, and heat strokes. Similar environments can also lead to loss of concentration, increased irritability and to excessive sweating, hence, decreasing these workers' productivity and efficiency at work (Miller and Bates, 2007). Moreover, hot conditions have been shown to increase the workers fatigue level, therefore, forcing them to increase their rest time and to decrease their working time, subsequently, resulting in a significant decrease in their output (Li et al., 2016). To improve outdoor work productivity, researchers focused on

the development of clothing capable of cooling the microclimate of the worker, and certain designs of cooling vests are already available commercially (Langø et al., 2009) to enhance the workers' tolerance of such environments (Caliskan et al., 2011). These cooling vests can be worn while performing the job, thus increasing the subjects' productivity and performance. Many different approaches and methods have been used to design cooling vests as different cooling processes are employed in the design. Those approaches include fluid cooling garments (FCGs), phase change materials (PCMs), and evaporative devices (Yang et al., 2012).

FCGs are based on the conductive heat exchange between the skin and a circulating cooling fluid (water, air or refrigerant). In the process of microclimate cooling, mechanical pumping is the force driving the circulation (Flouris and Cheung, 2006). The system relies on mechanical cooling, however, fluid pumping requires energy that reduces the efficiency of the system (Yang et al., 2012). On the other hand, PCM vests are equipped with cold packs of phase changing material, which can be any of the following: ice, salts, metallic or paraffin waxes. The vest depends on the melting of the packs, and therefore maintaining almost uniform surface temperature adjacent to the human trunk and cooling it (Itani et al., 2016; Mishra et al., 2015). PCM cooling vests are simple, functional, and relatively cheap; and they do not require a power supply system (Kenny et al., 2011). This makes them practical for workers in hot environments when physical activity is for limited periods of time. However, PCMs require energy for regeneration and a cool place to solidify after melting. Their added weight hinders moisture transport, and are sometimes flammable if made from paraffin.

Furthermore, the cooling effect of PCMs ends when the whole phase change material melts, this means that they are functional for a specific time duration (Mondal, 2008).

Evaporative techniques are passive techniques since they do not require substantial energy as the case of PCM and liquid circulating fluid. They can rely on water that is present in the inner layer material adjacent to the skin or on the sweat generated by the human body. The evaporative cooling vests consist of an evaporative microenvironment created between the layers of the cooling vest and the skin interacting with these layers. The sweat produced by the human skin is absorbed into highly hygroscopic materials. Afterwards, circulating air, supplied by the environment, evaporates the sweat, thus allowing for the cooling process. This takes advantage of the relatively significant latent heat of evaporation of water which is seven times larger than the latent heat of melting ice (Johnson, 2013) and at least ten times larger than that of common PCMs (Itani et al., 2017; Yazdi and Sheikhzadeh, 2014). These passive techniques use low-energy fans to facilitate the evaporation into the microclimate. Also, they have a long duration and they do not require the use of expensive coolants. Hence, this work will focus on developing an evaporative cooling vest.

Evaporative cooling techniques have been applied mainly on the human torso (Chinevere et al., 2008; Sun and Jasper, 2015; Xu and Gonzalez, 2011) since the areas of the torso, like the lower back, the upper back and the abdomen contribute mostly to the thermal comfort of the human body (Arens et al., 2006; Guéritée et al., 2015; Nakamura et al., 2008; Nakamura et al., 2013). Also, they have been applied to many different human resources including military personnel (Barwood et al., 2009) and

helicopter pilots (Reffeltrath, 2006). Previous evaporative models have incorporated direct evaporative cooling techniques for their vests. Xu and Gonzalez worked on a ventilation system that circulated the air around the torso into an air distribution garment (Xu and Gonzalez, 2011). Similarly, Chinevere et al. (2008) circulated air around the torso through the spacer vest liner. Using multiple fans, Sun and Jasper cooled the back by guiding entering air through an undergarment or a textile ribbon with the outlet airflow positioned at the top of the back and at its end (Sun and Jasper, 2015). The aforementioned models allow the air to flow in one direction and in a single channel in order to evaporate the sweat. However, this work aims to develop a new evaporative vest design to achieve a higher cooling capacity than the single channel one. The new vest design, used for cooling the back, would allow air to pass through a Maisotsenko cycle (M-cycle) (Mahmood et al., 2016) in which a dry and a wet channel are introduced.

The M-cycle is an evaporative cooling technique used in many cooling processes including air conditioning applications. The cycle allows the air to flow in counter directions of dry and wet channels, and the M-cycle was shown to be more efficient than the standard direct evaporative cooling method, leading to higher energy and moisture extractions (Al Touma et al., 2016; Anisimov et al., 2014; Itani et al., 2015; Mahmood et al., 2016; Pandelidis et al., 2016; Pandelidis and Anisimov, 2015; Younis et al., 2015). Thus, the advantage of the M-cycle vest is that it can achieve more cooling for the human skin by evaporating more water or sweat from the saturated inner fabric in contact with the human skin. The M-cycle works by allowing the inlet ambient

air to be sensibly cooled in the dry channel at a constant humidity ratio. Then, the air is evaporatively cooled by passing over wetted surfaces. This process allows the M-cycle to extract more energy and thus improve the cooling capacity of the vest. The M-cycle has successfully shown improvement when applied to heat exchangers and ceiling panels (Mahmood et al., 2016), but to the authors' knowledge, it has not been applied in vests to cool the back. It is therefore of interest to check its performance in cooling the human body. However, the proposed vest would be constrained by the back length of the human torso, as well as the choice of clothing for effective sweat capture and heat transfer. Moreover, the vest should be characterized by a light weight and provide comfort for the subject wearing it.

In this study, mathematical models for the M-cycle vest and the single channel vest for back-cooling are developed to compare and predict the cooling performance of the two vests, while making use of a wetted inner fabric placed adjacent to the skin. In addition, the two cooling vests are manufactured and experimented on to validate the developed models and compare their cooling performance at various air flow rates drawn from the ambient hot air. The models are validated experimentally using a heated plate placed in a hot climatic chamber. The validated M-cycle and single channel models are integrated with a bioheat model, developed by Karaki et al. (2013), to predict segmental skin temperature, core temperature and heat losses, and thus draw comparisons on the effect of the evaporative cooling designs on thermal comfort. Zhang's overall thermal sensation and comfort model is utilized to evaluate human thermal comfort state at determined conditions (Zhang et al., 2004). The integrated

model is used to assess the performance of the proposed M-cycle vest and its recommended conditions for use in terms of ambient conditions and human metabolic activity level.

B. System Description

The proposed M-cycle human back clothing system consists of two parallel channels: a dry channel and a wet channel, as shown in **Fig. 1**. The two channels are separated by a thin conductive fabric plate. Hot ambient air is introduced into the dry channel, where it flows and is sensibly cooled at a constant humidity ratio. The outlet air of the dry channel serves as the inlet of the wet channel. When air flows into the wet channel, it allows for the evaporative cooling process. The wet channel is heated from both sides due to the heat released by the human torso on one side and that gained from the air flowing in the dry channel on the other side.

The areas of the torso contribute mostly to the thermal comfort of the human body, much more than the limbs and extremities as the former possess thermal sensory that are more sensitive to cooling (Arens et al., 2006; Guéritée et al., 2015; Nakamura et al., 2008; Nakamura et al., 2013). This is why the M-cycle cooling vest is designed in this work to be placed on the back of the human body. The cooling vest is composed mainly of three fabric layers: an inner fabric sheet made of highly hygroscopic material, a middle conductive impermeable fabric layer and an outer insulation layer. The inner fabric layer of the cooling vest, which is in contact with the back skin, will be made of a hygroscopic material to retain the human sweat needed for evaporation. Ambient air is

drawn in by the battery-powered fan and forced to move downwards between the outer insulated surface and the middle conductive plate which form the dry channel of the cooling vest (see **Fig. 1**). The temperature decreases without any change in humidity (sensible cooling), and then it is guided to flow in the opposite direction between the inner hygroscopic fabric layer and the middle conductive layer which form the wet channel of the M-cycle (see **Fig. 1**). This causes an increase in the humidity of the flowing air. The water present in the hygroscopic material is evaporated into the air. The sensible cooling of the air prior to evaporation, is expected to increase the efficiency of the evaporative cooling garment. In order to maintain the form of the two channels and their structural stability, fabric spacers are installed along the channel length.

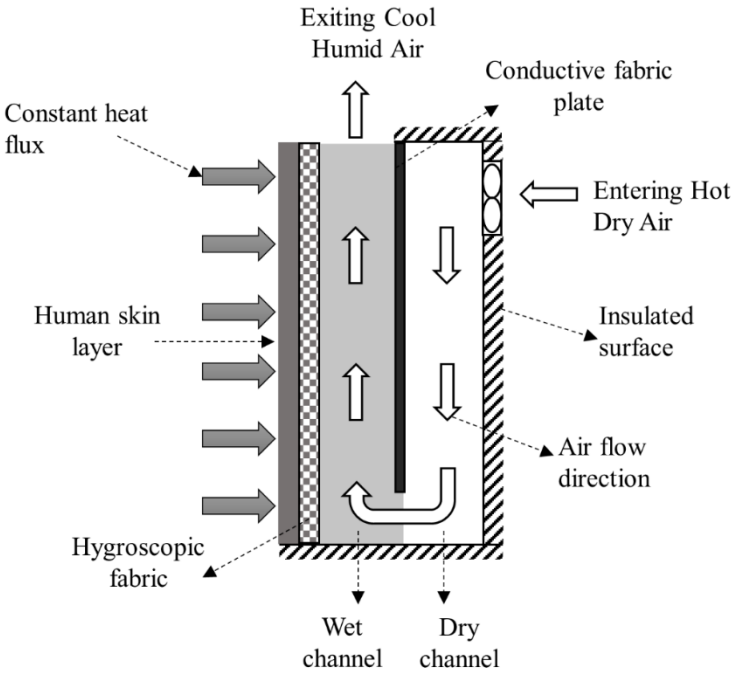

Fig. 1: Schematic showing a side view of the proposed M-cycle cooling vest

CHAPTER II

MATHEMATICAL MODELLING AND INTEGRATION WITH THE BIOHEAT MODEL

In this section, the development of the mathematical models for the M-cycle and single channel vests for cooling the back are presented, followed by their numerical methodology. The models are utilized to assess the cooling performance of the M-cycle design over the single channel one.

A. M-cycle Vest Model

A mass and heat transfer model of the three fabrics' interactions with the flowing air is developed to predict the performance of a cooling vest that incorporates the M-cycle with battery-operated ventilation fans. The cooling vest, as shown in **Fig. 2(a)**, is made up of the hygroscopic fabric thin layer in contact with the torso skin, the highly conductive fabric plate, the outer highly insulative fabric surface exposed to the ambient, and the dry and wet channels formed by the spacing between the fabric layers. The air flow driven by the fans, enters the vest at the upper torso clothed segments and moves downward through the dry channel and is then guided upward in the wet channel leaving the vest at the upper torso, as shown in **Fig. 2(a)**. The flowing air in the wet channel is designated as the microclimate air since it is adjacent to the human skin and inner hygroscopic fabric. A schematic of the psychrometric chart showing the processes of the single channel (in gray) and M-cycle (in black) models is presented in **Fig. 2(b)**. In single channel design, the air undergoes direct evaporative cooling and it gains

humidity while its temperature decreases (from 1 to 2'). In the M-cycle design, the air undergoes sensible cooling (from 1 to 2) at constant humidity ratio, then it is evaporatively cooled (from 2 to 3). The assumptions adopted in developing the M-cycle model are:

- The fabric layers are assumed thin justifying the use of simplified unidirectional mass and heat transfer.
- Axial conduction in the conductive fabric plate is neglected due to the high fabric conductivity.

The inner fabric made up of the hygroscopic material is treated as a surface fully saturated with water (Bachnak et al., 2018). This is justified as the fabric retains liquid sweat secreted by the back segments of a human, performing activity at high metabolic rate and the accumulated sweat, m_{acc}, is more than 35 g/m^2 (Ghali et al., 1995; Jones, 1992; Umeno et al., 2001; Wan and Fan, 2008). The hygroscopic fabric's temperature, T_{hf}, was assumed to be variable across the channel's length.

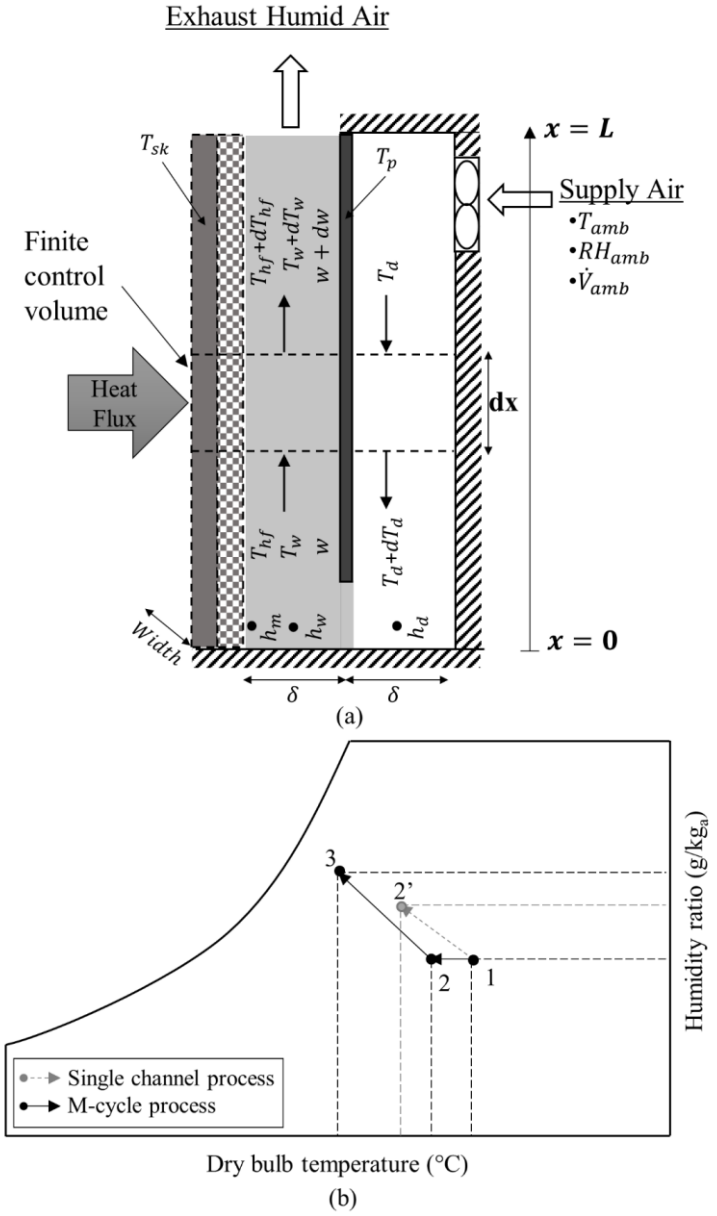

Fig. 2: Schematic showing (a) a finite control volume of the M-cycle model and (b) the single channel (in gray) and M-cycle (in black) processes on a psychometric chart

Dry channel energy balance

The specific enthalpy *h* of moist air is written as a function of both temperature and humidity ratio assuming constant specific heat of air such that:

$$h = Cp_a * T + h_{fg} * w \qquad (1)$$

where T is the temperature (°C), C_{pa} is the specific heat of air and w is the humidity ratio in the air (kg of H_2O/kg of dry air).

As the ambient is introduced into the dry channel, the air flows at constant humidity ratio, then the enthalpy change is a function of the temperature change only. Therefore, taking into consideration that the outside layer is completely insulated, the sensible heat balance in the dry channel is as follows:

$$\rho_d C_{pd} V \delta \frac{\partial T_d(x)}{\partial x} = h_d (T_p - T_d(\mathrm{x})) \qquad (2)$$

where x represents the axial coordinate along the air flow, δ the thickness of the channel, ρ the air density, V the flow velocity, T_d the dry channel air temperature that varies with x, and T_p the temperature of the conductive plate (see **Fig. 2(a)**).

Wet channel energy and mass balance (microclimate air)

On the other hand, the humidity ratio increases in the wet channel due to moisture gain, so the change in enthalpy can be calculated using the following relationship:

$$\frac{\partial h(x)}{\partial x} = Cp_a * \frac{\partial T_w(x)}{\partial x} + h_{fg} * \frac{\partial w(x)}{\partial x} \qquad (3)$$

However, the moisture gain in the wet channel is equal to the moisture exchange with the saturated inner fabric of the vest, as follows:

$$\rho_w V \delta \frac{\partial w(x)}{\partial x} = \left(\frac{P_{sat,T_{hf}}(x) - P_{air}(x)}{\frac{R_e h_{fg}}{2} + \frac{1}{2h_m}} \right) \qquad (4)$$

where w is the humidity ratio, $P_{sat,T_{hf}}$ is the saturation pressure of air at the hygroscopic fabric temperature, T_{hf}, P_{air} is the vapor pressure corresponding to the microclimate air in the wet channel, R_e is the evaporative resistance of the fabric, measured using a sweating guarded hot plate (ISO 11902) and h_m is the mass transfer coefficient that varies with the air flow velocity (Bachnak et al., 2018; Ghali et al., 1995). Equations (3) and (4) then lead to the following energy balance to find the temperature of the air inside the wet channel, T_w:

$$\rho_w C_{pw} V \delta \frac{\partial T_w(x)}{\partial x} = h_w\big(T_{hf}(x) - T_w(x)\big) + h_w(T_p - T_w(x)) \quad (5)$$

The energy balance in the middle layer was found by summing the two convective terms from each of its sides:

$$h_d\big(T_d(x) - T_p\big) + h_w\big(T_w(x) - T_p\big) = 0 \quad (6)$$

Inner hygroscopic fabric energy balance

The energy balance on the inner fabric layer is then written by including the conduction of the hygroscopic layer with the skin, the axial conduction in the hygroscopic layer and the convection with the air and the mass transfer term, as follows:

$$q"(x) - \delta * k_{hf} \frac{\partial^2 T_{hf}(x)}{\partial x^2} - h_w\big(T_{hf}(x) - T_w(x)\big) - h_{fg}\left(\frac{P_{sat,T_{hf}}(x) - P_{air}(x)}{\frac{R_e h_{fg}}{2} + \frac{1}{2h_m}}\right) = 0 \quad (7)$$

where $q"$, which is in W/m^2, is the constant heat flux boundary condition applied at the hygroscopic fabric and k_{hf} is the thermal conductivity of the hygroscopic fabric.

The variables in the models are therefore the air temperature variations in the dry and wet channels, the humidity ratio variation in the wet channel, the temperature variation of the hygroscopic fabric and the conductive plate's temperature.

B. Single Channel Evaporative Cooling Model

Considering the case of a single evaporative cooling channel, the channel is insulated at the layer exposed to the ambient and is subjected to a constant heat flux at the inner fabric layer. Thus, the heat balance equation for the air flowing in the evaporative channel is given by

$$\rho_w C_{pw} V \delta \frac{\partial T_w(x)}{\partial x} = h_w\left(T_{hf}(x) - T_w(x)\right) \quad (8)$$

The mass and energy balance equations on the hygroscopic sheet and remain the same as those presented above for M-Cycle.

C. Numerical Methodology

The equations that represent the heat and mass transfer processes inside the vest were discretized using the finite difference method over *N* elements with a discretization step Δx equal to 0.5 mm, as shown in Fig. 3. The discretization step was selected in such a way so that lower values had negligible effects on the solution of the equations. The number of grid points *N* is therefore equal to the vest length over the discretization step or $L/\Delta x$, which is the identical for the dry channel and the wet channel. The temperature of the hygroscopic sheet was assumed to be variable, therefore, the balance on the water sheet was solved at each element. The discretization was made such that:

$$T_{d(j+1)} = \frac{h_d \Delta x T_p + \rho_d C_{pd} V \delta T_{d(j)}}{h_d \Delta x + \rho_d C_{pd} V \delta} \quad (9)$$

$$T_{w(j+1)} = \frac{h_w \Delta x T_p + \rho_w C_{pw} V \delta T_{w(j)} + h_w \Delta x T_{hf(j+1)}}{\rho_w C_{pw} V \delta + 2 h_w \Delta x} \quad (10)$$

(10)

$$w_{(j+1)} = \frac{\Delta x \left(\frac{P_{sat}(T_{hf})(j+1) - P_{air(j+1)}}{\frac{R_e h_{fg}}{2} + \frac{1}{2h_m}} \right) + \rho_w V \delta w_{(j)}}{\rho_w V \delta} \quad (11)$$

The heat balance to find the uniform temperature of the highly conductive plate, T_p, is as follows:

$$T_p = \frac{h_d \sum_1^N (T_{d(j)+1} * \Delta x) + h_w \sum_1^N (T_{w(j+1)} * \Delta x)}{h_d * L + h_w * L} \quad (12)$$

Finally, using equation (7), for a constant heat flux boundary condition, the variation of the hygroscopic fabric temperature $T_{hf(j+1)}$ is given by:

$$T_{hf(j+1)} = \frac{q" + h_w T_w(j+1) + \frac{\delta * k_{hf}}{\Delta x^2} T_{hf}(j) - h_{fg} \left(\frac{P_{sat}(T_{hf})(j+1) - P_{air(j+1)}}{\frac{R_e h_{fg}}{2} + \frac{1}{2h_m}} \right)}{h_w + \frac{\delta * k_{hf}}{\Delta x^2}} \quad (13)$$

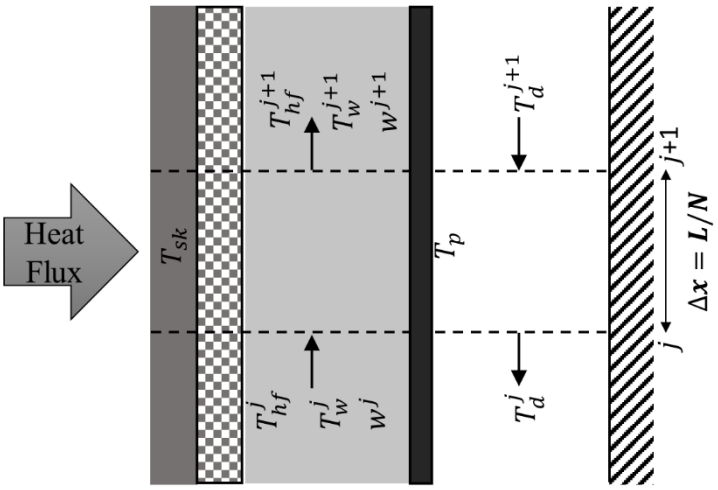

Fig. 3: Schematic showing the discretized control volume of the M-cycle model

The discretization boundary conditions were such that the temperature and humidity ratio of the inlet air at the first node, $j=N$, are those of the ambient air, and the

temperature and humidity ratio of the air leaving the dry channel (last node of the dry channel at *j=1*) were equal to the temperature and humidity ratio entering the wet channel, leading to continuity in mass and temperature. The model equations are solved iteratively until the solution of the different variables converged to an error less than 10^{-6}.

D. Integration with the Bioheat and Comfort Models

The multi-node segmental bioheat model of Karaki et al. (2013) allows the prediction of the segmental, mean skin, and core temperatures as well as the sweat rate under steady and transient activity levels and environmental conditions. The human body is divided into 27 segments to account for any physiological variation among the segments. The model divides the torso into four segments with eight skin nodes, each with a known surface area. In the integration, the distinct heat fluxes and skin temperatures of the upper and lower back segments are needed as boundary conditions for the vests' models. The inner fabric conditions of the back segments that are predicted by the vests' models are used to update the skin temperatures and skin vapor pressures of the back segments. Thus, the integration of the bioheat and vest models is done while ensuring continuity of heat and mass fluxes at the boundary between the skin surface and the inner fabric layer at any time. The detailed method of integration can be found in the work of Itani et al. (2017) and Bachnak et al. (2018). Overall thermal comfort is predicted using Zhang et al.'s model (2004) which is based on a scale varying from -4 (very uncomfortable) to +4 (very comfortable). The bioheat

model is integrated with both the single channel model and with the M-cycle model under the same ambient conditions and fan's flow rate. The comfort model is then used to check which model leads to higher comfort and improved thermal response to draw conclusions about the two designs.

In order to utilize the integrated model, an iterative solution was used to solve for the variation of the different parameters of the vests' models. Many different parameters were also needed for the bioheat model as input to be able to solve for the desired steady-state human body conditions. These parameters include the segmental metabolic rate, the ambient conditions (temperature and *RH*), the vest geometry and the fan flow rate. The iterative solution goes as follows: In order to calculate the inner fabric conditions, the skin temperature and vapor pressure are needed, along with the vests' dimensions and microclimate air mass flow rate provided by the fan. Then, mass and energy balance equations are used to predict at the new iteration the skin temperatures and vapor pressures of the back segments using the bioheat model. The iterations were continued until convergence occurred and the skin temperatures resulting from the bioheat model were equal to the ones predicted by the vests' models as shown in **Fig. 4**. The overall thermal comfort can then be predicted, once the segmental and mean skin temperatures and segmental and body core temperatures were found.

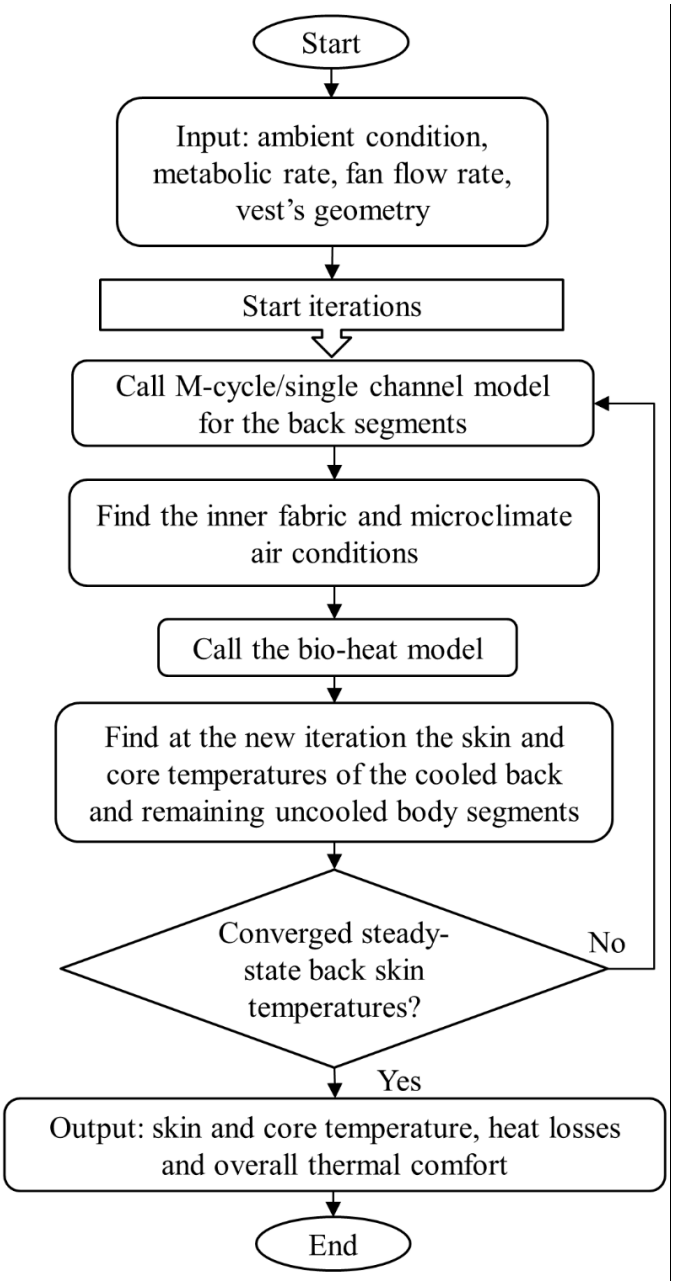

Fig. 4: Flow chart of the bioheat model sequence of operation.

The aim of this section is to utilize the integrated bioheat and M-cycle/single channel model and assess the cooling effect on human torso skin temperatures and on thermal comfort at moderate/hot ambient conditions and at different ambient *RHs*. Thus, the model predicts the conditions under which the M-cycle design improves vest

performance and when this performance is best with respect to thermal comfort as perceived by the subjects wearing it.

The simulation cases considered a human exposed for one hour to different outdoor ambient conditions while preforming a high activity at 6 MET (Jetté et al., 1990). The time for the inner fabric to attain saturation is short compared to the total activity period (Bachnak et al., 2018), thus, steady-state analysis of the results is possible. The studied ambient conditions were at 35 °C (moderate), 40 °C (hot) and 45 °C (very hot) at a constant ambient humidity ratio of 11.587 g/kg_a (see Table 1). The effect of *RH* on vest performance was also considered at three different *RHs* of 18 %, 25 % and 40 % only at the ambient temperature of 40 °C, since it represents a hot condition at which the body needs external cooling to dissipate any stored heat. The flow velocity induced by the fans in the vest was set to 0.8 m/s for all the simulated cases. The velocity was elected to be similar to those adopted in previous studies working with wearable evaporative cooling systems (Gebremedhin and Wu, 2001; Havenith et al., 2013; Lu et al., 2015; Sun and Jasper, 2015). These conditions mimicked working in outdoor conditions when heavy sweating would occur.

Table 1: **Simulation cases**

Cases	**Ambient temperature (°C)**	**Ambient humidity ratio (g/kg_a)**	**Ambient *RH* (%)**
1	40	8.300	18
2	40	11.587	25
3	40	18.749	40
4	35	11.587	33
5	45	11.587	19

CHAPTER III

EXPERIMENTAL METHODOLOGY AND VALIDATION

The aim of the conducted experiment is to compare the M-cycle design to the standard single channel direct evaporative cooling design while validating the mathematical model predictions. The experiments were conducted on a horizontal flat heated plate and simulations were done under boundary conditions similar to the ones subjected by the designed vests through the heated plate. Validation was done for the predicted outlet air temperature leaving the dry and wet channels, for the hygroscopic sheet temperature, and for the conductive plate temperature at three different air velocities of 0.8 m/s, 1.5 m/s and 2.3 m/s.

A. Cooling Vest Design and Setup

Two vest designs were manufactured in this study: i) a two-channel M-cycle vest, and ii) a direct evaporative cooling vest involving the simple one channel design. In the two vest designs, it is important to make sure that the velocity of the air flowing in the dry and wet channels is the same. This was done by having uniform spacing between the channels and between the fabric layers, along with adequate ventilation fans.

The outer insulation layer of the M-cycle vest was made of aerogel. Aerogel has been shown to have the best thermal insulation performance amongst solid materials (Jones, 1992). The used aerogel is composed of Cabot aerogel granules inside non-

woven fibers having a thermal conductivity equal to 23×10^{-3} W/m·K at room temperature. The material is flexible, highly insulative and lightweight and can operate with temperatures as high as 125 °C. Its fiber is composed of polyester and polyethylene. The middle layer of the M-cycle vest should be conductive and impermeable not only to successfully separate the dry and wet channels but also to allow heat transfer. Hence Adafruit's copper nanowire-based fiber material was selected. The material is composed of 70% polyester. Its thickness is 0.08 mm and its decomposing temperature is 200°C (Guo et al., 2013). The inner fabric sheet is required to be highly hygroscopic as it has to retain a significant amount of liquid. Cotton was selected because it has a high ability of holding moisture. The single channel vest, which served as a control design, was formed of the outer aerogel insulative layer and of the inner cotton fabric layer. Both samples are shown in **Fig. 5**.

Plexiglas bars were used as spacers to ensure constant microclimate air gap width and provide structural stability, thus maintaining the layers and the channels' thickness stable. Two spacers were used in each sample, thus forming three channels inside the vest. The measured channels' dimensions are such that its length (L) is 40 ± 0.05 cm, its width is 5.50 ± 0.05 cm and its thickness δ is 0.800 ± 0.005 cm. The air is introduced into the vests at different velocities, using three ventilation fans each having a diameter of 6 cm, corresponding to each channel. The air velocity was controlled by the voltage supply from the power supply to the fans. Thus, the air is set to flow uniformly between those spacers and across each channel. Moreover, multiple channels allow for taking measurements for each channel, increasing the number of recordings

that can be obtained at a time. The same channel design was applied for the M-cycle vest and the single channel one. The vests were placed such that the inner fabric was in contact with a heated plate. The heated plate was formed of a rectangular plate covered with 4 metallic resistance heaters Omega-KH-412 to produce a constant heat flux condition. Styrofoam insulation was used to insulate the bottom side of the heated plate and the sides of the vests along the channel length.

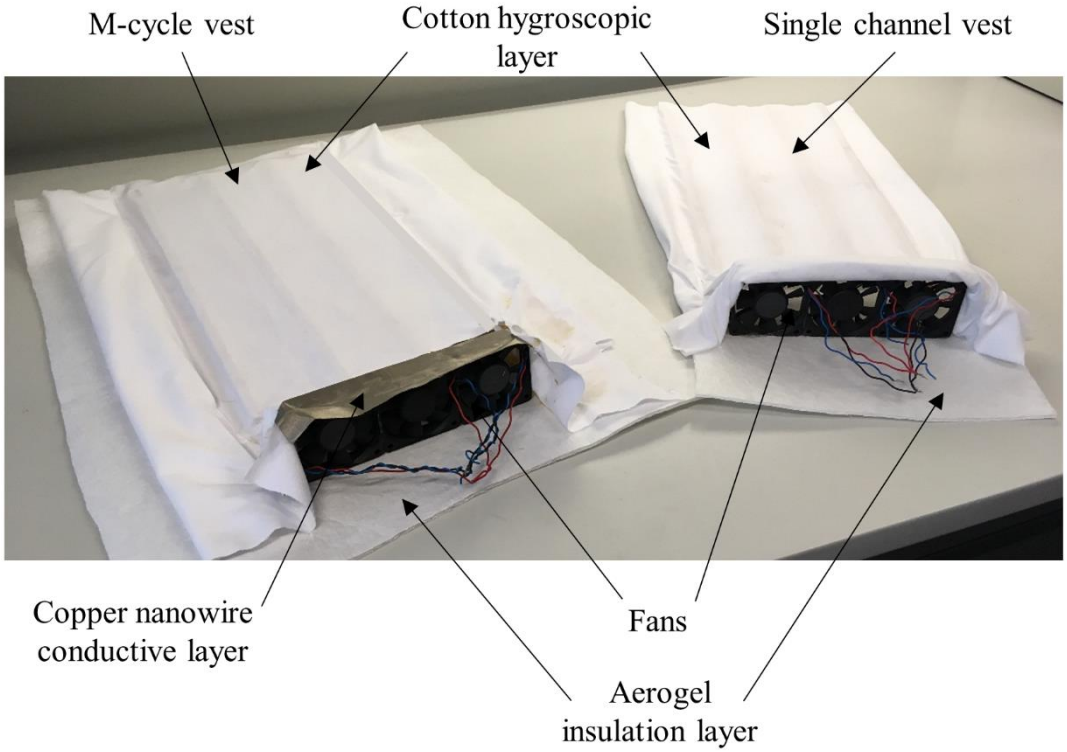

Fig. 5: Designs used in the experiments

B. Measurements and Protocol

The temperature and humidity of the ambient air in the climatic room were measured using a digital hygrometer and used as the input conditions for the air flow. The room was heated up until the conditions inside reached the stable required

temperature of 36 ± 0.5 °C and *RH* of 43 ± 2 %. The tests were done at three different input air velocities of 0.8 m/s, 1.4 m/s and 2.3 m/s. The air flow velocity at the outlet of the vest channel was measured using a hot wire anemometer (OMEGA HH2005HW, accuracy ± 5%). A schematic showing the front view of the experimental setup of M-cycle vest and measuring devices is presented in Fig. 6. Three sensors were set at the wet channels' exit to measure the temperature and *RH* of the leaving air. These sensors were iButton sensors (iButton® DS1923, Maxim Integrated) which have a -20 °C to 85 °C temperature operating range with a 0.5 °C error, and a 0 to 100% *RH* operating range with 0.04% error. Moreover, one T-type thermocouple of accuracy ± 0.1 °C was used to measure the air temperature at the middle of the wet channel. One T-type thermocouple was used to measure the air temperature at the outlet of the dry channel (inlet of wet channel). In addition, two T-type thermocouples were placed in contact with the hygroscopic sheet and another two thermocouples with the conductive plate to measure their respective temperature, as shown in Fig. 6. A digital precision balance (PGW3502, maximum reading of 3500 g and accuracy of 0.01 g) was used to monitor the weight loss of the whole setup to ensure steady-state saturation state of the inner fabric when measurements were taken.

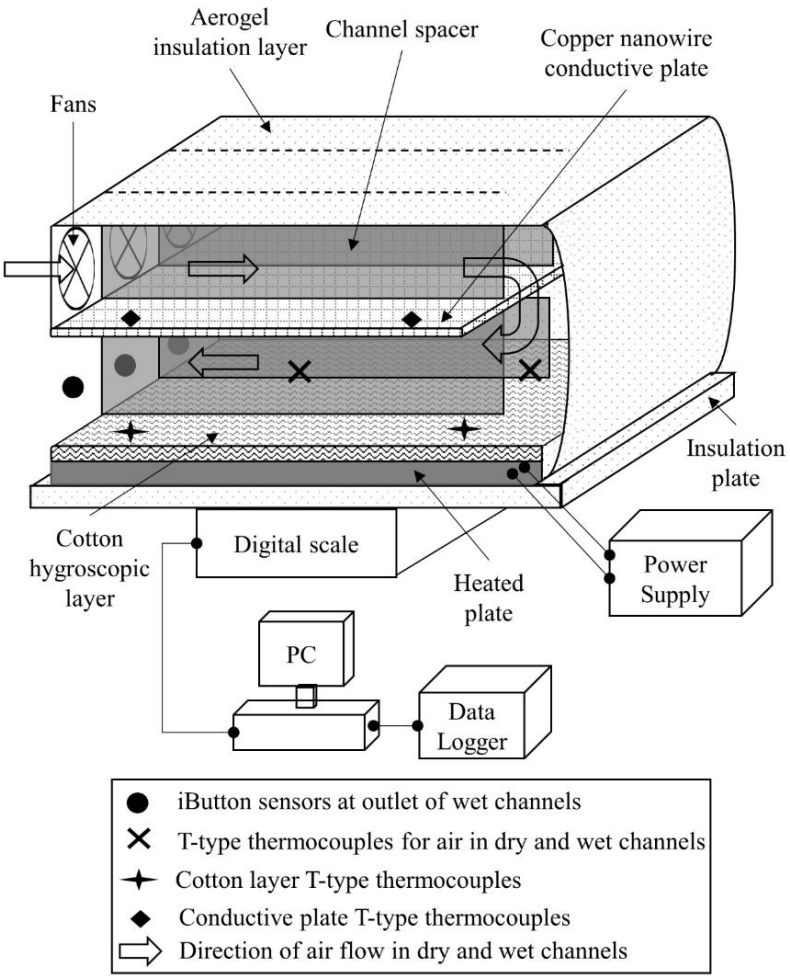

Fig. 6: Front view of the experimental setup of M-cycle vest and measuring devices

The procedure was applied to the M-cycle sample and to the standard direct evaporative cooling single-channel sample in a climatic chamber controlled at temperature of 36 ± 0.5 °C and 43 ± 2 % *RH*. One iButton sensor was placed at the end of each channel to measure the exiting air temperature and *RH* at a sampling rate of 10 seconds. The T-type thermocouples used to measure the air temperature at the outlet of the dry channels, the conductive plate temperature and the inner fabric or hygroscopic sheet temperature were set to take measurements at a sampling rate of 10 seconds. The

fabric temperature should be constant during the experiments so that the fabric is still at saturation.

At the beginning of the experiment, the heaters were turned on at the constant heat flux of 54.8 ± 1.5 W/m^2. The cotton inner fabric was fully wetted with water but without dripping and then it was placed in direct contact with the heaters covering their whole surface area. Then, for each flow rate, the fans were turned on for a total duration of 30 minutes, while data were being recorded. Finally, all the results were recorded every ten seconds and were extracted from the sensors for analysis and comparison with the model predictions at the three air velocities. Model predictions were obtained under similar ambient conditions and the results are then compared, to effectively validate the model first, and then determine the advantageous cooling of the M-cycle design.

C. Validation of the Mathematical Models

The single channel/M-cycle heated plate setup was simulated using the current developed model at the values of air flow velocities, heat flux, and dimensions of the channels. The inlet air temperature and *RH* to the single channel or to the dry channel of the M-cycle setup were equivalent to the experimental ambient conditions. The single channel/M-cycle models were simulated at the average air velocities of 0.8, 1.4 and 2.3 m/s. The steady-state model and experimental results of the wet air temperature at the inlet, middle and outlet of the wet channel, along with the humidity ratio at the outlet of the wet channel were analyzed. In addition, the hygroscopic fabric temperature at the inlet and outlet of the wet channel and the conductive plate temperature were examined.

A moisture balance of the experimental setup was first done in order to ensure that the moisture absorbed by the air flowing in the wet channel was equivalent to the mass of water evaporated from the wet hygroscopic fabric. The rate of moisture evaporation from the hygroscopic fabric was constant during that time, as well as the hygroscopic fabric temperature. In addition, an energy balance of the whole experimental setup was done. The energy input to the setup was the enthalpy of air entering the dry channel in the M-cycle setup or entering the single channel setup. The energy output was the enthalpy of air leaving the wet channel in the M-cycle setup or leaving the single channel setup. The resultant maximum errors for the mass and energy balances at the different air velocities are presented in Table 2 for the single channel and M-cycle setups.

Table 2: Maximum errors for the mass and energy balances at the different air velocities for the single channel and M-cycle setups

Air flow velocity (m/s)	**Cases**		***Maximum error* (%)**
0.8	Mass balance	Single channel	8.4
		M-cycle	7.4
	Energy balance	Single channel	8.3
		M-cycle	6.4
1.4	Mass balance	Single channel	8.6
		M-cycle	6.9
	Energy balance	Single channel	8.6
		M-cycle	8.1
2.3	Mass balance	Single channel	8.3
		M-cycle	8.2
	Energy balance	Single channel	7.1
		M-cycle	6.8

The model and experimental results of the wet air temperature along the length of the wet channel, at the different air flow velocities, are shown in Fig. 7(a) for the

single channel vest design and in Fig. 7(b) for the M-cycle design. The air flowing along the wet channel had a temperature drop, which varied at different air flow velocities for each of the vest designs. For example, at V=0.8 m/s, the temperature dropped from 36 ± 0.5 °C to 29.69 ± 0.58 °C in the single channel setup, whereas it dropped from 33.92 ± 0.32 °C to 27.58 ± 0.59 °C in the wet channel of the M-cycle setup. The temperature drop in the wet channel of the M-cycle setup was preceded by another temperature drop in the dry channel, where the entering air temperature was similar to that of the air entering the single channel (36 ± 0.5 °C). Thus, the air was cooled to a lower temperature in the M-cycle setup. Similar spatial variations of the air temperature were found at higher air flow velocities, however, higher temperatures were attained due to the air flowing at a faster rate with lower moisture gain and thus less cooling by evaporation. The single channel and M-cycle models showed accurate predictions of the spatial variation in the air temperature with maximum error of 4 % at the different air velocities.

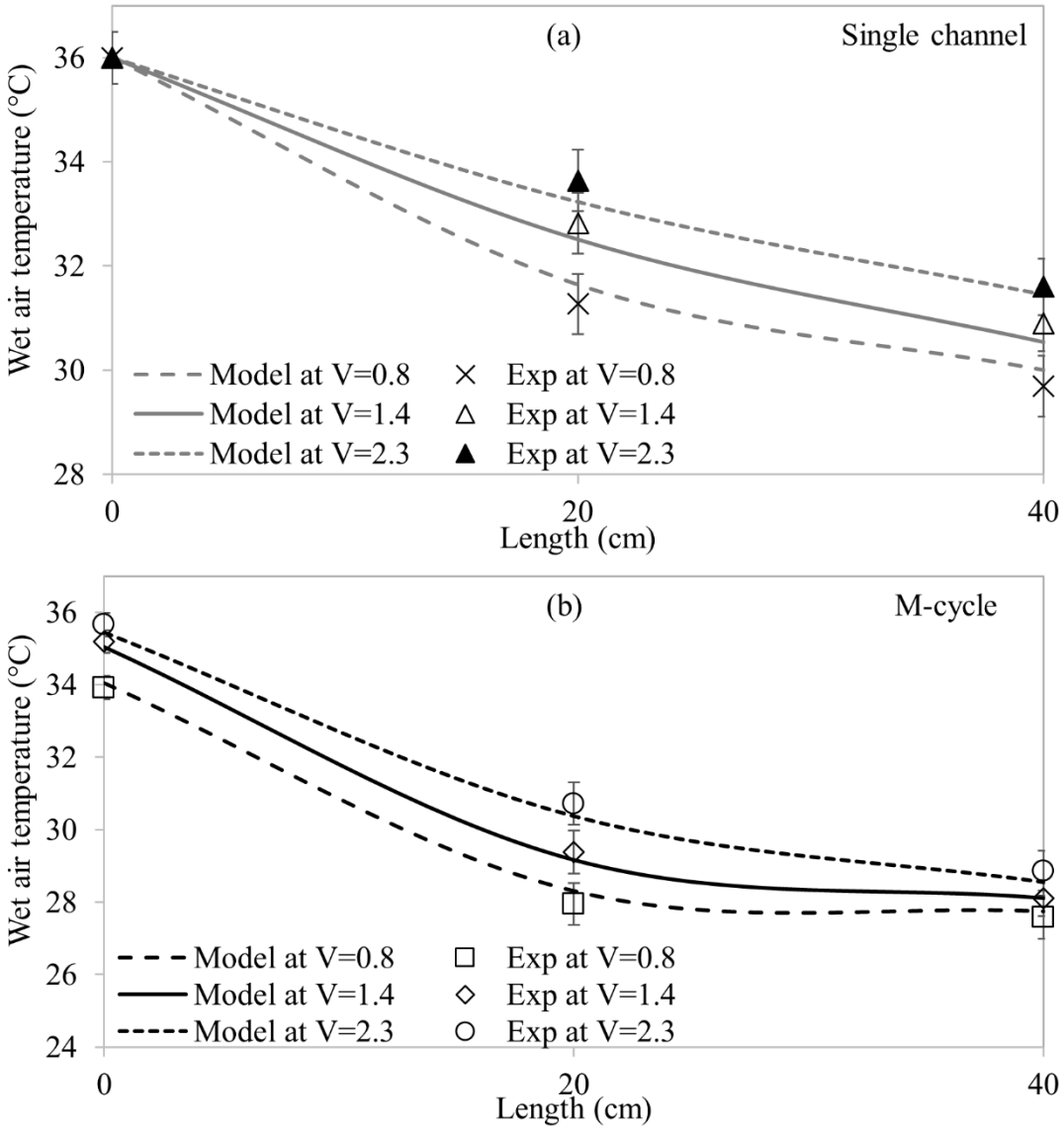

Fig. 7: The model and experimental results of the wet air temperature along the length of the wet channel, at different air flow velocities for (a) single channel and (b) M-cycle vest designs

Fig. 8 shows the model and experimental results of the wet air humidity ratio at the outlet of the wet channel, as a function of the air flow velocity for both vest designs. The input humidity ratio of the wet channel was 16.17 ± 0.77 g/kg$_a$, at the different air flow velocities. The humidity ratio of the flowing air in the wet channel increased due to moisture evaporated from the wet hygroscopic fabric. For example, at V=0.8 m/s the

humidity ratio increased to 19.96 ± 0.39 g/kg$_a$ in the single channel setup, whereas it increased to 20.92 ± 0.39 g/kg$_a$ in the M-cycle setup. Thus, the air gained more moisture in the M-cycle setup than the single channel one, which means more cooling of the fabric by evaporation. Similar moisture gains were found at higher air flow velocities, however, lower humidity ratios were attained since the air flowing at a faster rate was not able to gain as much moisture as compared to lower air velocities. The single channel and M-cycle models showed accurate predictions of the outlet air humidity ratio with maximum error of 6 % at the different air velocities.

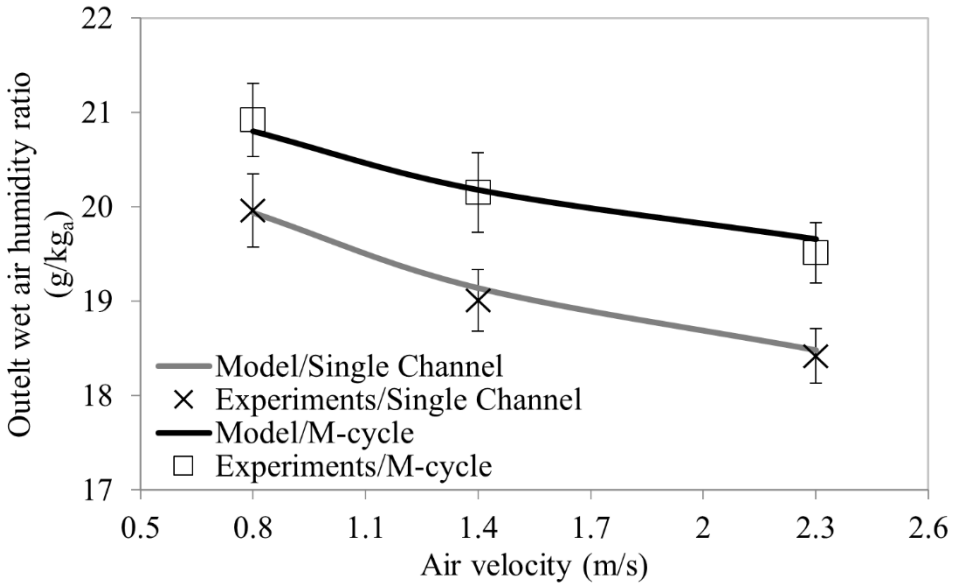

Fig. 8: The model and experimental results of the wet air humidity ratio at the outlet of the wet channel, as a function of the air flow velocity for both vest designs

Table 3 shows the model and experimental results of T_{hf} at the inlet and outlet of the wet channel for both vest designs, the average value of T_{hf}, and T_p for the M-cycle design, at different air flow velocities. The hygroscopic fabric temperature was affected by the flowing air that was cooled and gaining humidity along the length of the wet channel. For example, at V=0.8 m/s, T_{hf} decreased from 34.37 ± 0.40 °C (at inlet of

channel) to 30.05 ± 0.46 °C (at outlet of channel) in the single channel design. However, for the M-cycle design at V=0.8 m/s, T_{hf} decreased from 32.92 ± 0.41°C (at inlet of wet channel) to 27.65 ± 0.47 °C (at outlet of wet channel). T_{hf} had an increasing trend as the air flow velocity was increased from 0.8 to 2.3 m/s, in both vest designs, due to the reduced cooling by evaporation as discussed above. The single channel and M-cycle model predictions of T_{hf} showed good agreement with the experimental ones with maximum error of 6 % at the different air velocities. Regarding the conductive plate temperature, T_p, the results (see Table 3) showed that T_p increased from as the velocity increased from 30.96 ± 0.54 °C to 33.15 ± 0.45 °C, as the air velocity increased from 0.8 to 2.3 m/s. The maximum error in predicting T_p was 8 % at the different are velocities.

Table 3: Model and experimental results of T_{hf} at the inlet and outlet of the wet channel, average T_{hf} and T_p at different air flow velocities

Air flow velocity (m/s)	**Cases**		**T_{hf} at inlet of wet channel (°C)**	**T_{hf} at outlet of wet channel (°C)**	**Average T_{hf} (°C)**	**T_p (°C)**
0.8	Single channel	Model	34.65	29.83	31.97	-
		Experiment	34.37±0.40	30.05±0.46	32.02±0.44	-
	M-cycle	Model	33.12	27.32	28.92	31.36
		Experiment	32.92±0.41	27.65±0.47	29.12±0.45	30.96±0.54
1.4	Single channel	Model	35.61	30.46	32.55	-
		Experiment	35.44±0.42	30.54±0.48	30.50±0.45	-
	M-cycle	Model	34.22	27.9	29.61	32.46
		Experiment	33.95±0.40	28.25±0.47	29.96±0.44	32.79±0.56
2.3	Single channel	Model	35.89	31.04	33.20	-
		Experiment	35.78±0.42	30.9±0.51	33.10±0.45	-
	M-cycle	Model	34.59	28.41	30.49	32.78
		Experiment	34.52±0.45	28.58±0.32	30.66±0.38	33.15±0.45

The above results show that the single channel and M-cycle vest models were able to accurately predict the spatial variation of the air temperature along the wet

channel, and the corresponding humidity ratio at the outlet, at different air velocities. The models were also capable of predicting the variation of the hygroscopic fabric temperature and the conductive plate temperature at different air flow velocities. The results also showed that the M-cycle vest design was capable of cooling the hygroscopic fabric to lower temperatures than the single channel design, due to higher moisture absorption by the flowing air and cooling by evaporation, at the different air velocities. This can be further explained by the schematic of the psychometric chart shown in Fig. 9, which presents the process undergone at V=0.8 m/s for the single channel (in gray) and the M-cycle (in black) models. More evaporation was present in the M-cycle setup, which is indicated by the higher outlet humidity ratio of the air in the wet channel leading to lower fabric temperatures. The M-cycle vest was able to attain lower fabric temperatures more significantly at lower air velocities than the single channel one, as indicated by the average values of T_{hf}. As shown in Table 3, at V=0.8 m/s, average T_{hf} was 32.02 ± 0.44 °C in the single channel design, while it was 29.12 ± 0.45 °C in the M-cycle one.

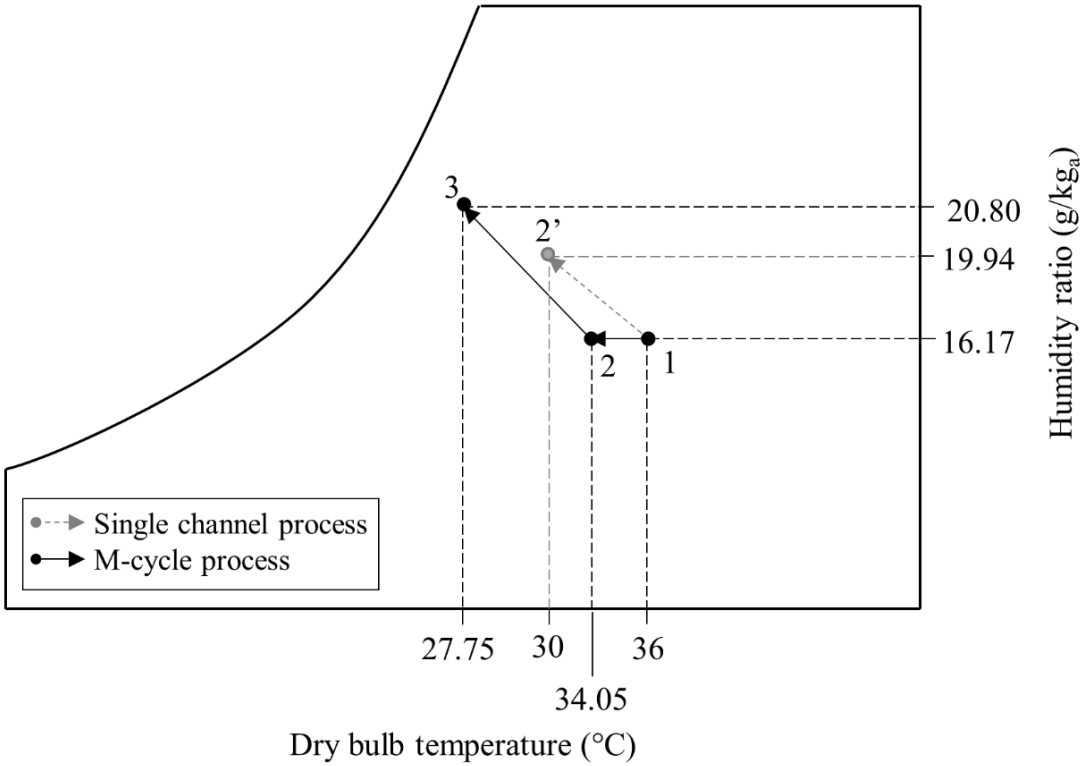

Fig. 9: Schematic of the psychometric chart showing the process at V=0.8 m/s for single channel (in gray) and M-cycle (in black) models

CHAPTER IV

RESULTS AND DISCUSSION

The thermal state of upper body parts contribute mostly to the overall thermal comfort of the human (Guéritée et al., 2015; Nakamura et al., 2013). Thus, using the validated M-cycle/single channel model integrated with the bioheat model, the performance of the proposed vest designs in cooling the back can be assessed for a human performing heavy activity at 6 MET (Jetté et al., 1990). First, the effect of ambient *RH* on back torso skin temperature, $T_{back,torso}$, and overall thermal comfort was studied at constant ambient temperature of 40 °C. Then, the effect of ambient temperature was analyzed at constant ambient humidity ratio of 11.587 g/kg_a. The selected velocity of the air flow in the vests was V= 0.8 m/s, since it showed lower air and hygroscopic fabric temperatures, as described in the validation section. Previous studies also showed that as the air flow rate or air velocity increases, the attained air temperatures in the dry and wet channels decreased (Pandelidis and Anisimov, 2015; Zhan et al., 2011). Moreover, the conditions at which the M-cycle vest showed the highest improvement over the single channel one are analyzed.

A. Impact of Ambient Relative Humidity

The simulation results of the steady-state back torso skin temperature, $T_{back,torso}$, under the single channel and M-cycle vest designs, at varying ambient *RH* from 18 % to 40 % and constant hot ambient temperature of 40 °C, are shown in Fig. 10(a). The corresponding results of overall thermal comfort are also shown in Fig. 10(b). As the ambient *RH* increased and became more humid, $T_{back,torso}$ increased in both vest designs,

since the ability of the human body to release heat by sweat evaporation decreases. Consequently, the overall thermal comfort decreased and the human was getting more uncomfortable, as shown in Fig. 10(b). However, the M-cycle vest design was able to attain lower $T_{back,torso}$ than the single channel one, and thus improved thermal comfort at all ambient *RHs*. The M-cycle vest showed lower $T_{back,torso}$ by 1.27 °C, 1.15 °C and 0.93 °C, at ambient *RH* of 18 %, 25 % and 40 %, respectively, with improved corresponding thermal comfort by 38 %, 27 % and 15 %. It can be noticed that the M-cycle vest showed more significant improvements over the single channel one at lower ambient *RHs*, which implies the benefit of evaporative cooling.

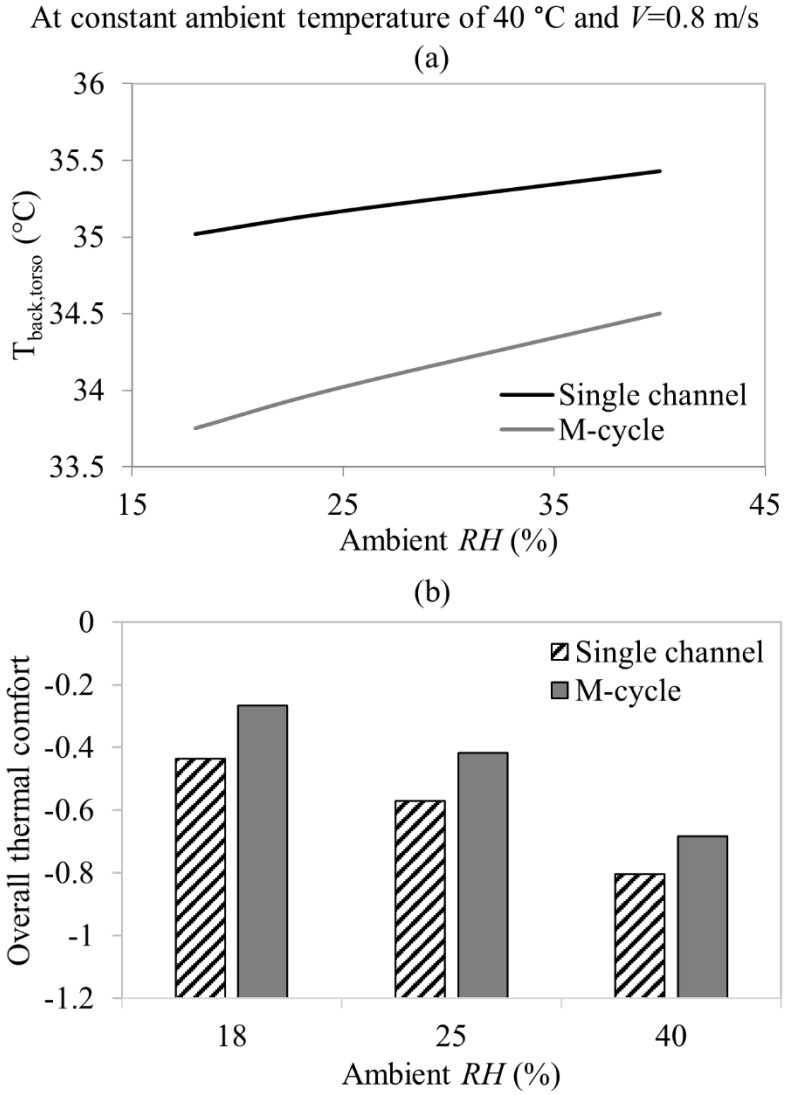

Fig. 10: Plots showing the (a) back torso skin temperature and (b) corresponding overall thermal comfort, under the single channel and M-cycle vest designs at different ambient *RHs*, constant ambient temperature of 40 °C and *V*= 0.8 m/s

B. Impact of Ambient Temperature

The simulation results of $T_{back,torso}$ under the single channel and M-cycle vest designs, at varying ambient temperature from moderate (35 °C) to very hot (40 °C) and constant moderate ambient humidity ratio of 11.587 g/kg$_a$, are shown in Fig. 11(a). The corresponding results of overall thermal comfort are also shown in Fig. 11(b). As the

ambient temperature increased from moderate to very hot, $T_{back,torso}$ increased slightly in both vest designs. In addition, the overall thermal comfort decreased since the human body was getting hotter, as shown in Fig. 11(b). However, the M-cycle vest design showed lower $T_{back,torso}$ than the single channel one, and thus improved thermal comfort at all ambient temperatures. The M-cycle vest showed lower $T_{back,torso}$ by 1.02 °C, 1.15 °C and 1.26 °C, at ambient temperature of 35 °C, 40 °C and 45 °C, respectively, with improved corresponding thermal comfort by 26 %, 27 % and 29 %. Thus, the improvement in the performance of the M-cycle vest over the single channel one was more noticeable at higher ambient temperatures due to the higher cooling effect of sweat evaporation.

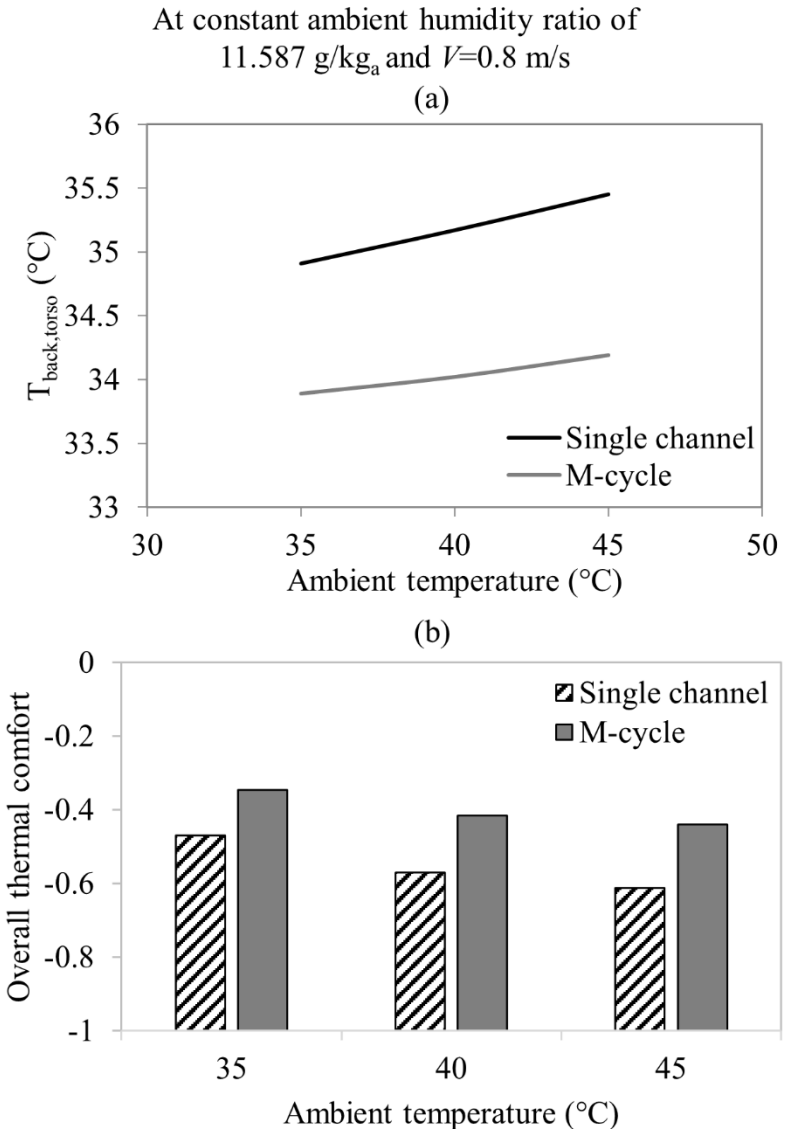

Fig. 11: Plots showing the (a) back torso skin temperature and (b) corresponding overall thermal comfort, under the single channel and M-cycle vest designs at different ambient temperatures, constant ambient humidity ratio of 11.587 g/kg$_a$ and V= 0.8 m/s

The above results show that adopting the M-cycle vest design, over the conventional single channel one, was effective in facilitating body cooling by sweat evaporation at high activity level of 6 MET. The vest design was able to make use of the secreted sweat to provide further cooling to the human torso and improve thermal comfort levels at different ambient conditions. The results also showed that the

proposed M-cycle vest was more effective at lower ambient *RHs* and higher ambient temperatures. Further testing of the proposed vest can be done on human subjects to show the practicality of the vest, keeping in mind that the presence of sweat is a key factor for the vest cooling capacity. In addition, manufacturing of a wearable vest that should ensure proper sweat capture, torso coverage and air flow is needed.

C. Conclusion

The current study suggested a cooling vest that is placed on the back and that is based on the indirect evaporative cooling technique; the M-cycle. This technique cools sensibly the inlet ambient air in a dry channel before it is evaporatively cooled in a wet channel. The study has developed mathematical models for both the proposed M-cycle vest design and the standard single channel direct evaporative cooling technique. Two vests mimicking the designs were fabricated in order to conduct experiments and validate the developed models. The experimental setup comprised of a heated plate that provides these vests with a constant heat flux boundary condition. The experiments have validated the mathematical models and showed that the M-cycle design was extracting more moisture from the hygroscopic fabric leading to lower fabric temperature compared to the standard direct evaporative cooling vest. The spatial variation of the air temperature in the wet channel, the air humidity ratio, the fabric temperature and the M-cycle plate temperature were also measured during the experiments in order to make sure that the mathematical models were consistent across all of their results.

A validated bioheat model was integrated with the validated vest models to compare the effect of the two vests on the thermal and comfort responses of workers subject to high physical activities in different outdoor conditions. The M-cycle design was able to reduce the torso skin temperature and thus, to enhance the overall comfort of the workers more than the single channel one. The M-cycle design showed better improvements at relatively higher ambient temperature of 45°C and lower relative humidity of 18%. Future work might need to test the M-cycle design on thermal manikins or on actual human subjects. Also, future research might try to integrate the M-cycle vest with different applications and types of activities.

BIBLIOGRAPHY

- Al Touma A, Ghali K, Ghaddar N, Ismail N. Solar chimney integrated with passive evaporative cooler applied on glazing surfaces. Energy. 2016;115:169-79.
- Anisimov S, Pandelidis D, Danielewicz J. Numerical analysis of selected evaporative exchangers with the Maisotsenko cycle. Energy Conversion and Management. 2014;88:426-41.
- Arens E, Zhang H, Huizenga C. Partial- and whole-body thermal sensation and comfort - Part II: Non-uniform environmental conditions. Journal of Thermal Biology. 2006;31(1-2):60-6.
- Bachnak R, Itani M, Ghaddar N, Ghali K. Performance of Hybrid PCM-Fan Vest with Deferred Fan Operation in Transient Heat Flows from Active Human in Hot Dry Environment. Building and Environment. 2018;144:334-348.
- Barwood MJ, Newton PS, Tipton MJ. Ventilated vest and tolerance for intermittent exercise in hot, dry conditions with military clothing. Aviation Space and Environmental Medicine. 2009;80(4):353-59.
- Caliskan H, Hepbasli A, Dincer I, Maisotsenko V. Thermodynamic performance assessment of a novel air cooling cycle: Maisotsenko cycle. International Journal of Refrigeration. 2011;34(4):980-90.
- Chinevere TD, Cadarette BS, Goodman DA, Ely BR, Cheuvront SN, Sawka MN. Efficacy of body ventilation system for reducing strain in warm and hot climates. European Journal of Applied Physiology. 2008;103(3):307-14.
- Flouris AD, Cheung SS. Design and Control Optimization of Microclimate Liquid Cooling Systems Underneath Protective Clothing. Annals of Biomedical Engineering. 2006;34(3):359-72.
- Gebremedhin KG, Wu B. A model of evaporative cooling of wet skin surface and fur layer. Journal of Thermal Biology. 2001;26(6):537-45.
- Ghali K, Jones B, Tracy J. Modeling heat and mass transfer in fabrics. International Journal of Heat and Mass Transfer. 1995;38(1):13-21.
- Guéritée J, House JR, Redortier B, Tipton MJ. The determinants of thermal comfort in cool water. Scandinavian Journal of Medicine & Science in Sports. 2015;25(5):e459-71.
- Guo H, Lin N, Chen Y, Wang Z, Xie Q, Zheng T, et al. Copper nanowires as fully transparent conductive electrodes. Scientific Reports. 2013;3:2323-30.
- Havenith G, Bröde P, Hartog ED, Kuklane K, Holmer I, Rossi RM, et al. Evaporative cooling: effective latent heat of evaporation in relation to evaporation distance from the skin. Journal of Applied Physiology. 2013;114(6):778-85.
- ISO 11902: Textiles—physiological effects—measurement of thermal and water-vapor resistance under steady-state conditions sweating guarded-hotplate test-1993. Geneva, Switzerland.
- Itani M, Ghaddar N, Ghali K, Ouahrani D, Chakroun W. Cooling vest with optimized PCM arrangement targeting torso sensitive areas that trigger comfort

when cooled for improving human comfort in hot conditions. Energy & Buildings. 2017;139:417-25.
- Itani M, Ghali K, Ghaddar N. Performance Evaluation of Displacement Ventilation System Combined with a Novel Evaporative Cooled Ceiling for a Typical Office in the City of Beirut. Energy Procedia. 2015;75:1728-33.
- Itani M, Ouahrani D, Ghaddar N, Ghali K, Chakroun W. The effect of PCM placement on torso cooling vest for an active human in hot environment. Building and Environment. 2016;107:29-42.
- Jetté M, Sidney K, Blümchen G. Metabolic equivalents (METS) in exercise testing, exercise prescription, and evaluation of functional capacity. Clinical Cardiology. 1990;13(8):555-65. doi:10.1002/clc.4960130809.
- Johnson JK. Evaluation of Four Portable Cooling Vests for Workers Wearing Gas Extraction Coveralls in Hot Environments. ProQuest Dissertations Publishing; 2013.
- Jones BW, Ogawa Y. Transient interaction between the human and the thermal environment. ASHRAE Transactions. 1992;98:189-195.
- Karaki W, Ghaddar N, Ghali K, Kuklane, K, Holmér, I, Vanggaard, L. Human thermal response with improved AVA modeling of the digits. International Journal of Thermal Sciences. 2013;67:41-52.
- Kenny G, Schissler A, Stapleton J, Piamonte M, Binder K, Lynn A, et al. Ice Cooling Vest on Tolerance for Exercise under Uncompensable Heat Stress. Journal of Occupational and Environmental Hygiene. 2011;8(8):484-91.
- Langø T, Nesbakken R, Færevik H, Holbø K, Reitan J, Yavuz Y, Mårvik R. Cooling vest for improving surgeons' thermal comfort: A multidisciplinary design project. Minimally Invasive Therapy & Allied Technologies. 2009;18(1):20-9.
- Li X, Chow KH, Zhu Y, Lin Y. Evaluating the impacts of high-temperature outdoor working environments on construction labor productivity in China: A case study of rebar workers. Building and Environment. 2016;95:42-52.
- Lu Y, Wei F, Lai D, Shi W, Wang F, Gao C, Song G. A novel personal cooling system (PCS) incorporated with phase change materials (PCMs) and ventilation fans: An investigation on its cooling efficiency. Journal of Thermal Biology. 2015;52:137-46.
- Mahmood MH, Sultan M, Miyazaki T, Koyama S, Maisotsenko VS. Overview of the Maisotsenko cycle – A way towards dew point evaporative cooling. Renewable and Sustainable Energy Reviews. 2016;66:537-55.
- Miller VS, Bates GP. The Thermal Work Limit Is a Simple Reliable Heat Index for the Protection of Workers in Thermally Stressful Environments. Annals of Occupational Hygiene. 2007;51(6):553-61.
- Mishra A, Shukla A, Sharma A. Latent heat storage through phase change materials. Resonance. 2015;20(6):532-41.
- Mondal S. Phase change materials for smart textiles – An overview. Applied Thermal Engineering. 2008;28(11):1536-1550.

- Nakamura M, Yoda T, Crawshaw LI, Kasuga M, Uchida Y, Tokizawa K, et al. Relative importance of different surface regions for thermal comfort in humans. European Journal of Applied Physiology. 2013;113(1):63-76.
- Nakamura M, Yoda T, Crawshaw LI, Yasuhara S, Saito Y, Kasuga M, et al. Regional differences in temperature sensation and thermal comfort in humans. Journal of Applied Physiology. 2008;105(6):1897-1906.
- Pandelidis D, Anisimov S, Worek WM, Drąg P. Numerical analysis of a desiccant system with cross-flow Maisotsenko cycle heat and mass exchanger. Energy & Buildings. 2016;123:136-50.
- Pandelidis D, Anisimov S. Numerical analysis of the heat and mass transfer processes in selected M-Cycle heat exchangers for the dew point evaporative cooling. Energy Conversion and Management. 2015;90:62-83.
- Reffeltrath PA. Heat stress reduction of helicopter crew wearing a ventilated vest. Aviation Space and Environmental Medicine. 2006;77(5):545-50.
- Sun Y, Jasper WJ. Numerical modeling of heat and moisture transfer in a wearable convective cooling system for human comfort. Building and Environment. 2015;93:50-62.
- Umeno T, Hokoi S, Takada S. Prediction of skin and clothing temperatures under thermal transient considering moisture accumulation in clothing/ Discussion. ASHRAE Transactions. 2001;107:71.
- Wan X, Fan J. A transient thermal model of the human body-clothing-environment system. Journal of Thermal Biology. 2008;33:87-97.
- Xu X, Gonzalez J. Determination of the cooling capacity for body ventilation system. European Journal of Applied Physiology. 2011;111(12):3155-60.
- Yang Y, Stapleton J, Diagne BT, Kenny GP, Lan CQ. Man-portable personal cooling garment based on vacuum desiccant cooling. Applied Thermal Engineering. 2012;47:18-24.
- Yazdi M M, Sheikhzadeh M. Personal cooling garments: a review. The Journal of The Textile Institute. 2014;105(12):1231-50.
- Yi W, Chan A. Effects of Heat Stress on Construction Labor Productivity in Hong Kong: A Case Study of Rebar Workers. International Journal of Environmental Research and Public Health. 2017; 14(9).
- Younis M, Ghali K, Ghaddar N. Performance evaluation of the displacement ventilation combined with evaporative cooled ceiling for a typical office in Beirut. Energy Conversion and Management. 2015;105:655-64.
- Zhan C, Duan Z, Zhao X, Smith S, Jin H, Riffat S. Comparative study of the performance of the M-cycle counter-flow and cross-flow heat exchangers for indirect evaporative cooling - Paving the path toward sustainable cooling of buildings. Energy. 2011;36(12):6790-805.
- Zhang H, Huizenga C, Arens E, Wang D. Thermal sensation and comfort in transient non-uniform thermal environments. European Journal of Applied Physiology. 2004;92(6):728-33.